Microsc. Microanal. 18, 808–815, 2012
doi:10.1017/S1431927612000402

Microscopy AND Microanalysis

Deconvolution of Calcium Fluorescent Indicator Signal from AFM Cantilever Reflection

G. Monserratt Lopez-Ayon,[1,*] David J. Oliver,[1] Peter H. Grutter,[1] and Svetlana V. Komarova[2,3]

[1]*Center for the Physics of Materials and the Department of Physics, McGill University, 3600 University, Montreal, Quebec H3A 2T8, Canada*
[2]*Shriners Hospital for Children, Montreal, Quebec, Canada*
[3]*Faculty of Dentistry, McGill University, Montreal, Quebec, Canada*

Abstract: Atomic force microscopy (AFM) can be combined with fluorescence microscopy to measure the changes in intracellular calcium levels (indicated by fluorescence of Ca^{2+} sensitive dye fluo-4) in response to mechanical stimulation performed by AFM. Mechanical stimulation using AFM is associated with cantilever movement, which may interfere with the fluorescence signal. The motion of the AFM cantilever with respect to the sample resulted in changes of the reflection of light back to the sample and a subsequent variation in the fluorescence intensity, which was not related to changes in intracellular Ca^{2+} levels. When global Ca^{2+} responses to a single stimulation were assessed, the interference of reflected light with the fluorescent signal was minimal. However, in experiments where local repetitive stimulations were performed, reflection artifacts, correlated with cantilever motion, represented a significant component of the fluorescent signal. We developed a protocol to correct the fluorescence traces for reflection artifacts, as well as photobleaching. An added benefit of our method is that the cantilever reflection in the fluorescence recordings can be used for precise temporal correlation of the AFM and fluorescence measurements.

Key words: AFM, fluorescence artifacts, mechanical stimulation, calcium signaling, fluo-4

Introduction

The development of atomic force microscopy (AFM) has enabled investigations of a wide range of samples and environments, from single atom manipulation in ultra-high vacuum to studies of individual molecules, proteins, nucleic acids, and different structures of living cells in buffered solutions (Muller, 2008). AFM imaging is fundamentally different from conventional microscopy in that it allows localized, highly controlled invasion and manipulation of nano- and microscopic structures. These qualities have rendered it a technique of wide application in biology. Combining AFM with fluorescence microscopy, a technique widely used in biology, provides simultaneous ability to locally manipulate the sample (such as in force spectroscopy and nanomanipulation techniques) and to visualize the associated dynamic changes in cell status, properties, or signaling as reported by labeled molecules (Barfoot et al., 2008; Oh et al., 2008; Sanchez et al., 2010). The combined setup enables a complementary examination of the sample and a better understanding of the physiological processes than either of the techniques alone can deliver. However, it is important to understand potential interactions between different instruments and be prepared for the possibility of artifacts in the measurements.

Received February 2, 2012; accepted March 2, 2012
*Corresponding author. E-mail: lopezm@physics.mcgill.ca

AFM imaging allows local, controlled, and quantifiable mechanical or chemical interactions with the cellular and molecular structures, which enables experiments that require high-resolution imaging, determination of local mechanical properties, or the application of mechano-chemical stimuli. These techniques involve the use of a tip integrated at the very end of a cantilever. Interactions between the tip and the sample are controlled by the deflection of the cantilever. Thus, during experiments the tip moves relative to the sample to perform the measurement. The AFM application of particular interest to us is its use to study cell sensitivity to mechanical deformation of cell membranes (Charras & Horton, 2002; Ehrlich & Lanyon, 2002; Guo et al., 2006). One of the most prominent first cellular responses to mechanical stimulations of different nature is transient elevation of cytosolic free calcium concentration ($[Ca^{2+}]_i$) (Duncan & Turner, 1995). Several fluorophores have been developed and successfully used to study changes in $[Ca^{2+}]_i$, including fura-2, fluo-3, and fluo-4 (Molecular Probes, 2011). Fluo-3 and -4 can be used in situations where only a visible spectrum excitation light source is available, and fluo-4 is brighter and more stable when compared to fluo-3 (Molecular Devices, 2010). Our goal was to establish a combined AFM and fluorescence microscopy setup to measure the changes in $[Ca^{2+}]_i$ (indicated by fluorescence of fluo-4-loaded osteoblastic cells) in response to mechanical stimulation performed by AFM. Since mechanical stimulation using AFM is associated with cantilever movement, we hypothesized that this motion may potentially interfere with the fluorescence signal.

Materials and Methods

Mechanical Stimulation of a Single Cell Using AFM

C2C12 cells stably transfected with BMP-2 were kindly provided by M. Murshed, McGill University. Cells were cultured in Dulbecco's Modified Eagle Medium (DMEM from Invitrogen Corporation, Carlsbad, CA, USA) supplemented with 2 mM of L-glutamine, 100 IU of penicillin, 100 μg/mL of streptomycin, and 10% of fetal bovine serum (Wisent, Inc., Montreal, Quebec, Canada) on round 25 mm No. 1 glass coverslips (Warner Instruments, Hamden, CT, USA) at 5% CO_2 at 37°C. The media were changed every third day. Cells were cultured to 50–70% confluence to allow easy identification of individual cells. The experiments were conducted using an MFP-3D-BIO AFM (Asylum Research, Santa Barbara, CA, USA) mounted on an Olympus IX-71 inverted optical microscope. The sample placed in the closed fluid cell was left undisturbed for 15 min to achieve thermal equilibrium at 37°C. A 60× oil immersion objective with 1.45 NA (Olympus, Tokyo, Japan) was put into contact with the coverslip allowing optical access from the bottom and AFM probe access from the top of the sample. The region of interest over the nucleus of the cell was located and aligned with the cantilever tip using bright-field and fluorescence images. Cells were mechanically stimulated using an NCLAuD cantilever (Nanosensors, Neuchatel, Switzerland), with a spring constant (k) of 40 ± 8 N/m. The tip end was etched to a 1 μm^2 area using a focused ion beam microscope (FEI DB235; FEI Company, Hillsboro, OR, USA) to have a well-defined truncated pyramid shape, allowing the local pressure to be determined. The cantilever deflection and distance the probe moved were monitored and plotted in a deflection-distance curve. The force ($F = k \cdot deflection$), the range (the net extension of the piezo element in a deflection-distance curve), the speed, and the number of indentations were controlled.

Intracellular Calcium Measurements

The cells were loaded with 0.7 μM (micromolar) concentration of Ca^{2+}-sensitive dye Fluo4–AM (Molecular Probes, Eugene, OR, USA) in culture media for 40 min at room temperature. The dye was washed twice with physiological buffered solution (130 mM NaCl; 5 mM KCl; 10 mM glucose; 1 mM $MgCl_2$; 1 mM $CaCl_2$; 20 mM) containing 2% 1 M HEPES (pH 7.4) (Kemeny-Suss et al., 2009), the coverslip was assembled on to the peak fluid chamber (Asylum Research) and physiological buffered solution (1.5 mL) was added. The cells were illuminated with a 488 nm argon laser, and the emitted light was collected with a charge-coupled device camera (Cascade II; liquid from Photometrics, Tucson, AZ, USA). In each experiment 200 images were acquired in a sequence. The exposure time was set to 250 ms and minimum time between frames was selected. The average time per frame was calculated to be 335 ± 10 ms.

Analysis

Data are presented as representative traces, representative images, or means ± standard error of the mean. AFM data were acquired using the Igor Pro software package; fluorescence images were collected using Image-Pro Plus (Version 6.2.) and saved as *.tif files. Matlab was used to extract, combine, and analyze fluorescence intensity data, calculate the fast Fourier transform (FFT), and analyze the power spectrum. Power spectra peaks were fitted using least-squares regression to a power law. Fluorescence and force spectroscopy measurements were correlated using Igor Pro.

Results

Experimental Setup

Calcium (Ca^{2+}) signaling has been shown to be the prominent first response of osteoblastic cells to any type of mechanical stimulation (Hung et al., 1995, 1996; Chen et al., 2000). As a model of osteoblastic cells, we used the C2C12 cell line stably transfected with BMP-2 and cultured for 2–6 days (Li et al., 2011). Cells exhibiting osteoblastic morphology (strongly adhered mono-nucleated cells with relatively large body and several filopodia) were chosen for mechanical testing. Post-experiment, the cells were fixed and stained for osteoblast marker alkaline phosphatase. Cells exhibiting osteoblastic morphology were also stained positive for the alkaline phosphatase (Fig. 1A). Mechanical stimulation was performed with AFM force spectroscopy using a 1 μm^2 diameter tip. We analyzed Ca^{2+} transients in response to two different regimes of mechanical stimulation: (1) low load indentation in which only membrane deformation was induced (Figs. 1B, 1C, green trace) and (2) high load indentation in which the membrane was penetrated after deformation (Figs. 1B, 1C, blue trace). The membrane penetration event is easily identifiable on the deflection-distance curve as a decrease in the force required to continue to move the probe.

Photobleaching of Fluo-4 Fluorescence

Because $[Ca^{2+}]_i$ transients are elicited in response to mechanical stimulation, we used Ca^{2+}-sensitive fluorescent dye Fluo-4-AM (Molecular Probes, 2011) to study Ca^{2+} responses to mechanical stimulation. First, to assess photobleaching, we monitored Fluo-4-loaded cells for the period required to perform the indentation experiment. Photobleaching was evident as a decrease in fluorescence intensity in the field of observation over time (Fig. 2A). The cells in the field of view were individually selected with the assistance of bright-field imaging (Fig. 2A, white ellipses), and the average intensity for each cell was plotted as a function of the frame (Fig. 2B solid lines). As described by Vicente and colleagues (Vicente et al., 2007), the traces were fitted with a mono-exponential decay $I(t) = Ae^{-at}$ function, resulting in $a = 228 \pm 28$ s (Fig. 2B, dotted lines). Photobleaching was also evident in the experiments where mechanical stimulation was induced (Figs. 2C–2F). When high load indentation resulting in membrane deformation and penetration was induced (Fig. 2C), the cell exhibited a global increase in fluorescence intensity, indicating a $[Ca^{2+}]_i$ transient (Fig. 2D). When the cells were indented with

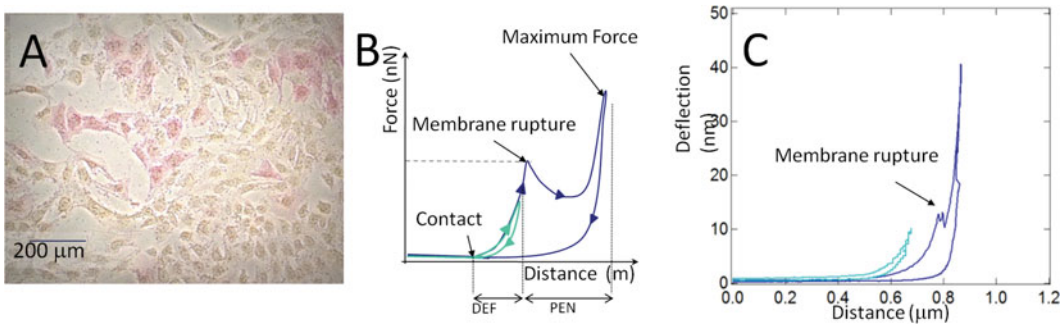

Figure 1. Testing mechanosensitivity of bone cells using AFM. C2C12 cells stably transfected with BMP-2 were cultured for 2–6 days to obtain an osteoblastic phenotype. **A:** Representative image of C2C12 culture stained for osteoblast marker, alkaline phosphatase (red). **B**, **C:** A single cell was indented using a cantilever with a blunt tip of 1 μm^2 (square micrometers). The force exerted by the probe and the distance the probe moves were monitored and plotted as a deflection-indentation curve. **B:** Schematic representation of events observed using deflection-force curve: (a) the contact point of the tip is evident as increase in force required to move the probe; (b) when membrane rupture force is reached, the tip penetrates the cell (apparent by a decrease in the cell resistance); (c) when a predetermined maximum force is reached probe retraction is initiated. The maximum force was set to be either below (green) or above (blue) the membrane rupture force. DEF is the extent of membrane deformation; PEN is the depth of probe penetration. **C:** Examples of deflection-distance curves from experiments in which membrane deformation only (green) or deformation plus penetration (blue) were induced.

forces leading to membrane deformation only (Fig. 2E), the cell exhibited local elevations in fluorescence intensity, which were only apparent at the point of contact with the indenting tip (Fig. 2F). Multiple increases in fluorescence intensity were observed in response to multiple consecutive stimulations (Fig. 2F).

The Movement of AFM Cantilever Affects Sample Illumination

During analysis of the experiments in which multiple consecutive membrane deformations at 0.1 Hz were performed, we noticed regular oscillations of the background signal (Supplementary Movie 1).

Supplementary Movie 1

Supplementary Movie 1 can be found online. Please visit journals.cambridge.org/jid_MAM.

We plotted the average intensity over an ellipse surrounding the total area of the stimulated cell (cell 1) and nonstimulated cells (cells 2–4) as a function of time (Fig. 3A). Changes in fluorescence intensity of nonstimulated cells are synchronized with those in the stimulated cell; therefore, it is unlikely that these changes are biological in nature. The characteristic frequencies of the fluorescence signal of the nonstimulated cells were assessed using FFT, and the peak frequency of the power spectrum was found to be 0.128 ± 0.001 Hz (Fig. 3B). The deflection curves were plotted as a function of time, and the average duration of each indentation was found to be ~8 s, resulting in a frequency of 1/8 = 0.125 Hz, which closely corresponds to the oscillation frequency in fluorescence traces (Fig. 3C). Next, for the experiments performed at different indentation speeds, the peak frequency of the fluorescence intensity traces was calculated and plotted as a function of the average duration of a corresponding deflection curve. A $f = 1/t$ relation was obtained by fitting a power function to the dataset ($R^2 = 0.998$) (Fig. 3D). Thus, the frequency (f) of the oscillations observed in fluorescence traces corresponds to a period ($1/f$) with which the indentations were performed. We concluded that the motion of the AFM cantilever affects the sample illumination due to reflection of laser light from the cantilever, producing changes in the fluorescence intensity of nonstimulated cells that are unrelated to changes in the $[Ca^{2+}]_i$ of stimulated cells, as schematically summarized on Figure 3E.

Protocol for Signal Correction for Bleaching and Cantilever Reflection

To correct for the cantilever motion and bleaching artifacts, raw fluorescence traces were processed using Matlab (Supplementary Information 1, Matlab code 1).

Supplementary Information 1

Supplementary Information 1 (SupInfII) can be found online. Please visit journals.cambridge.org/jid_MAM.

The image sequence was loaded into the program, and ellipses surrounding different cells were manually selected (Figs. 4A, 4D). The spatially-averaged intensity for each selected cell was calculated for each frame, and the frame evolution of the average fluorescence intensity was plotted (Figs. 4 B, 4E).

For the experiments in which global increase in fluorescence intensity (an average intensity higher than fourfold the average noise) was observed (Figs. 4A–4C), the curves were processed as follows (Supplementary Information 2, Matlab code II).

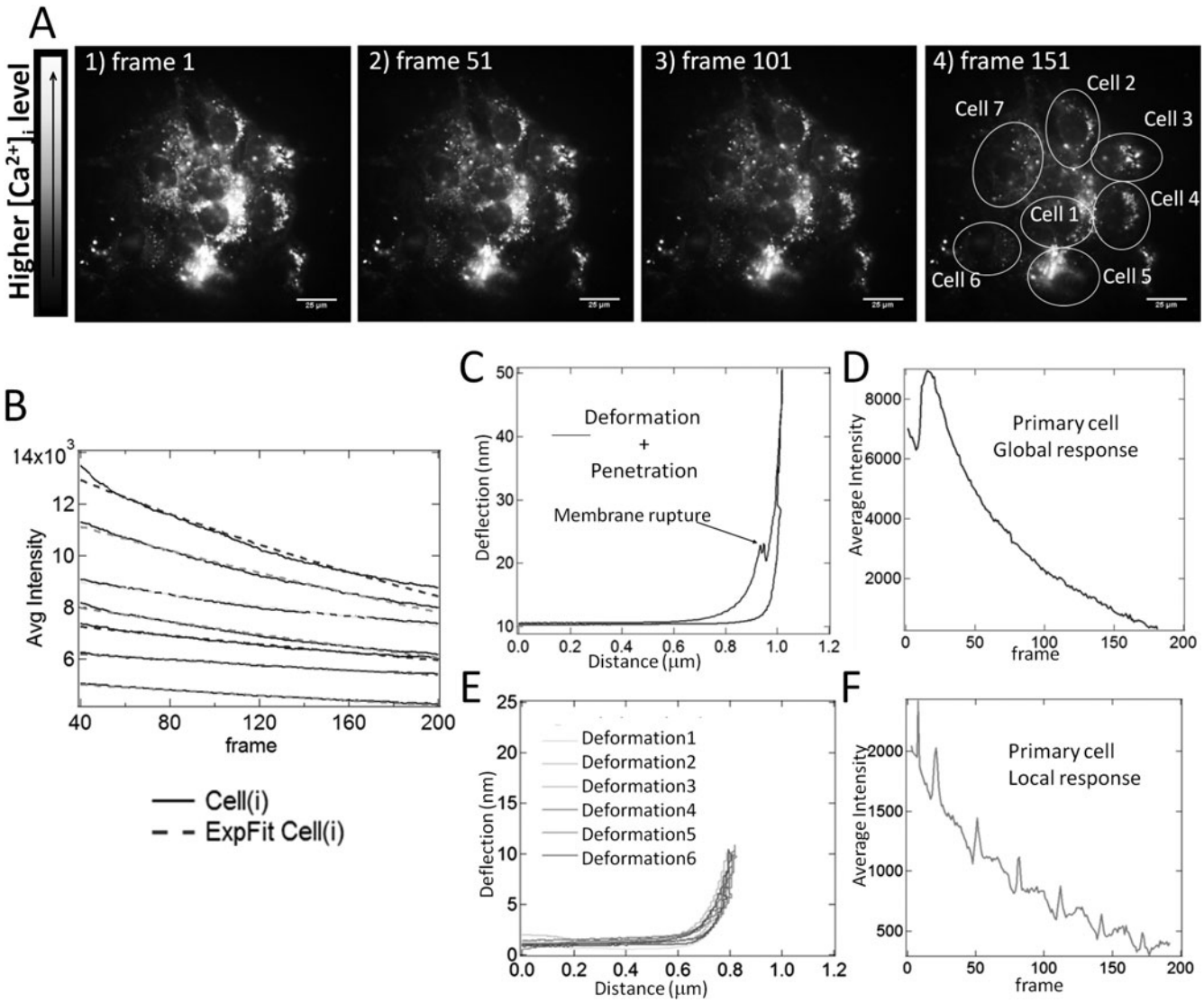

Figure 2. Photobleaching of the calcium-sensitive fluorescent indicator fluo-4 AM. **A**, **B:** Osteoblastic cells were loaded with 0.7 μM (micromolar) concentration of Ca^{2+}-sensitive dye Fluo4 AM and changes in fluorescence intensity over time were assessed. **A:** Overall decrease in fluorescent intensity is evident over the image sequence taken at ~3 frames/s. No mechanical stimulation was performed. Image frames are indicated at each image. Scale bar is 25 μm in all images. Different cells were identified with the assistance of bright-field image and are indicated by white ellipses. **B:** The average fluorescence intensity of each cell was determined and plotted as a function of frame (solid traces). The intensity trace of each cell was fitted with a mono-exponential decay function (dotted lines). **C–F:** Photobleaching is evident in fluorescence traces acquired while mechanical stimulation was performed. **C**, **D:** Deformation leading to membrane rupture induced global increase in fluorescence intensity. **C:** Deflection-distance curve of stimulation leading to membrane rupture. **D:** The average fluorescence intensity over the total area of indented cell was plotted as a function of frame. **E**, **F:** Low level membrane deformation induced local increase in fluorescence intensity. **E:** Deflection-distance curves for the six consecutive stimulations performed in the same position in a single cell. **F:** The average fluorescence intensity over a 5 μm diameter circle centered at the indentation site was plotted as a function of frame.

Supplementary Information 2

Supplementary Information 2 (SuplInfGlobal) can be found online. Please visit journals.cambridge.org/jid_MAM.

First, we assessed if the changes in fluorescence intensity could be due to changes in sample illumination. We assume that changes in sample illumination are evident in the fluorescence traces of nonstimulated cells; therefore, if we can find a linear combination of the fluorescence profiles of the n nonindented cells $Cell(i)$ ($\sum_{i=2}^{n=1} a(i) \cdot Cell(i)$) such that the Primary cell profile will be obtained, then the increase in fluorescence intensity in the Primary cell is due to changes in sample illumination and not in $[Ca^{2+}]_i$. If the Primary trace (Fig. 4C) and the linear combination (Fig. 4C)

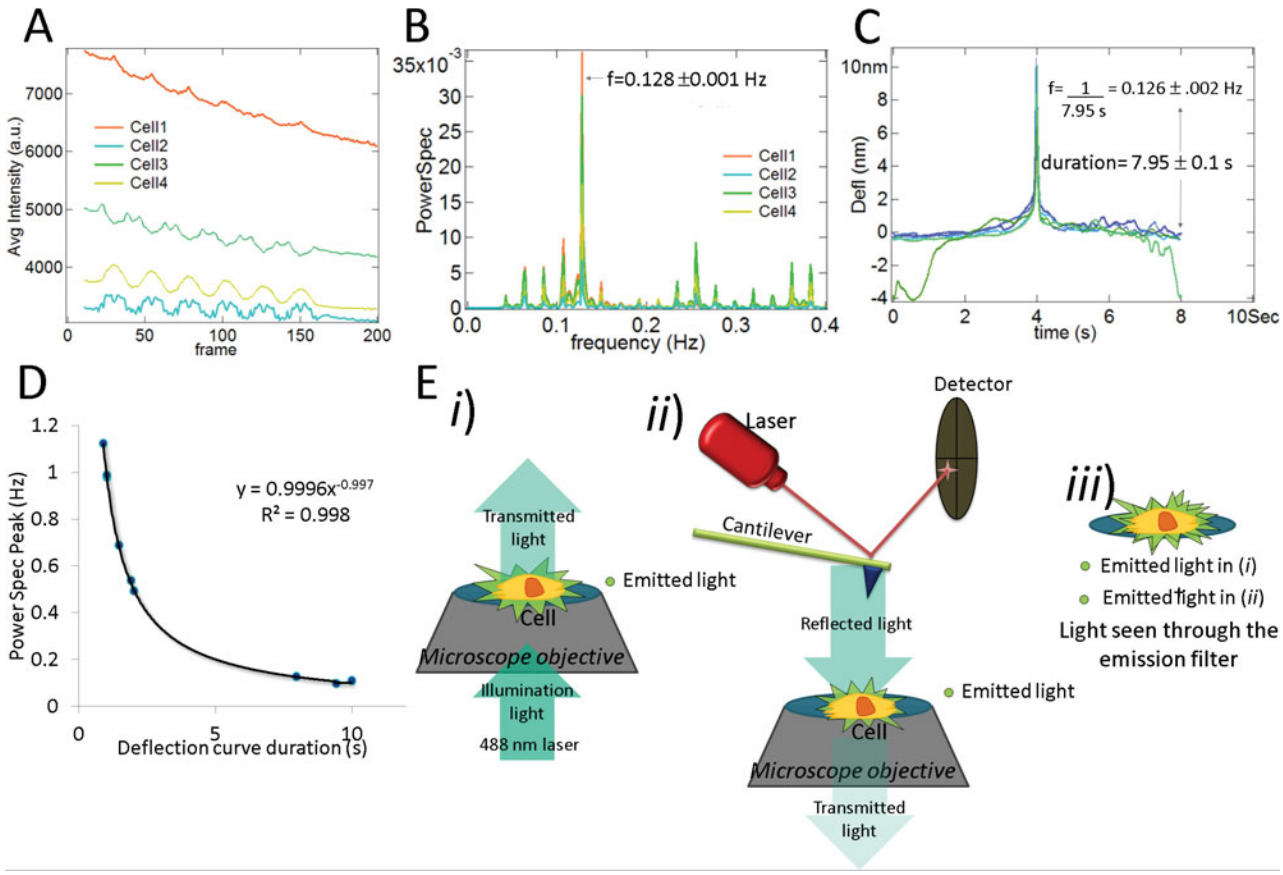

Figure 3. Motion of the AFM cantilever affects sample illumination resulting in changes in fluorescence intensity unrelated to changes in $[Ca^{2+}]_i$. Osteoblastic cells were loaded with Fluo4 AM and changes in fluorescence intensity in response to multiple consecutive AFM stimulations were assessed in stimulated and nonstimulated cells. **A:** The average fluorescence intensity over the total area of indented cell (cell 1) or nonstimulated cells (cell 2–4) was plotted as a function of frame. Oscillatory fluorescence intensity changes in nonstimulated cells are evident. **B:** The Power spectrum (PowSpec) of the FFT for each cell trace in panel **A** was calculated and is plotted as a function of the frequency. A frequency peak appears at 0.128 ± 0.001 Hz. **C:** The deflection-time curves acquired for the same experiment are plotted as a function of time. **D:** The power spectrum was calculated for nonstimulated cells in experiments performed at different indentation speeds, the peak frequency of the power spectrum for each experiment is plotted as a function of the duration of the deflection-time curves. A power fit was calculated and a relation $\sim 1/f$ was obtained with $R^2 = 0.998$. **E:** Schematics of the effect of the presence of the cantilever on the sample illumination: (*i*) The incident light in the sample is partially absorbed by the sample and partially transmitted through the sample (green arrow). The fluorophores that absorbed light at the excitation wavelength are now excited and decay back to their lower energy state, emitting light at a longer wavelength (emitted light in *i*). (*ii*) The light transmitted continues its optical path and is then reflected by the cantilever, which is located a few microns above the sample. The back-reflected light is again partially absorbed by the sample, and thus more fluorophores are excited emitting additional light (emitted light in *ii*). (*iii*) The light emitted by the fluorophores is detected (emitted light in *i* + emitted light in *ii*).

are different, specifically at the peak of the fluorescence increase, it can be concluded that the Primary cell exhibited a Global Ca^{2+} response to mechanical stimulation.

Next we corrected the Global Ca^{2+} response for photobleaching. A new linear combination of nonstimulated cells (Fig. 4C, ExtrLinComb) was fitted to the initial (before stimulation) and final (last 25 frames of recording) extremes of the Global response trace (Fig. 4C), and approximated with a mono-exponential decay curve (Fig. 4C, ExpFit). Global trace was divided by the ExpFit curve resulting in the final bleaching-corrected (i.e., normalized) Global Ca^{2+} response (Fig. 4C, UnbGlobal). Although we sometimes see reflection artifacts in stimulated and nonstimulated cells, in all cases they appear before the onset of global Ca^{2+} response. Therefore, when the post-stimulation time frame is selected for analysis, no additional procedure is required to correct for these artifacts in the experiments with global calcium responses.

For the experiments in which multiple consecutive low load membrane deformations were performed (Figs. 4D–4F), the traces were processed as follows (Supplementary Information 3, Matlab code III).

Supplementary Information 3

Supplementary Information 3 (SuplInfLocal) can be found online. Please visit journals.cambridge.org/jid_MAM.

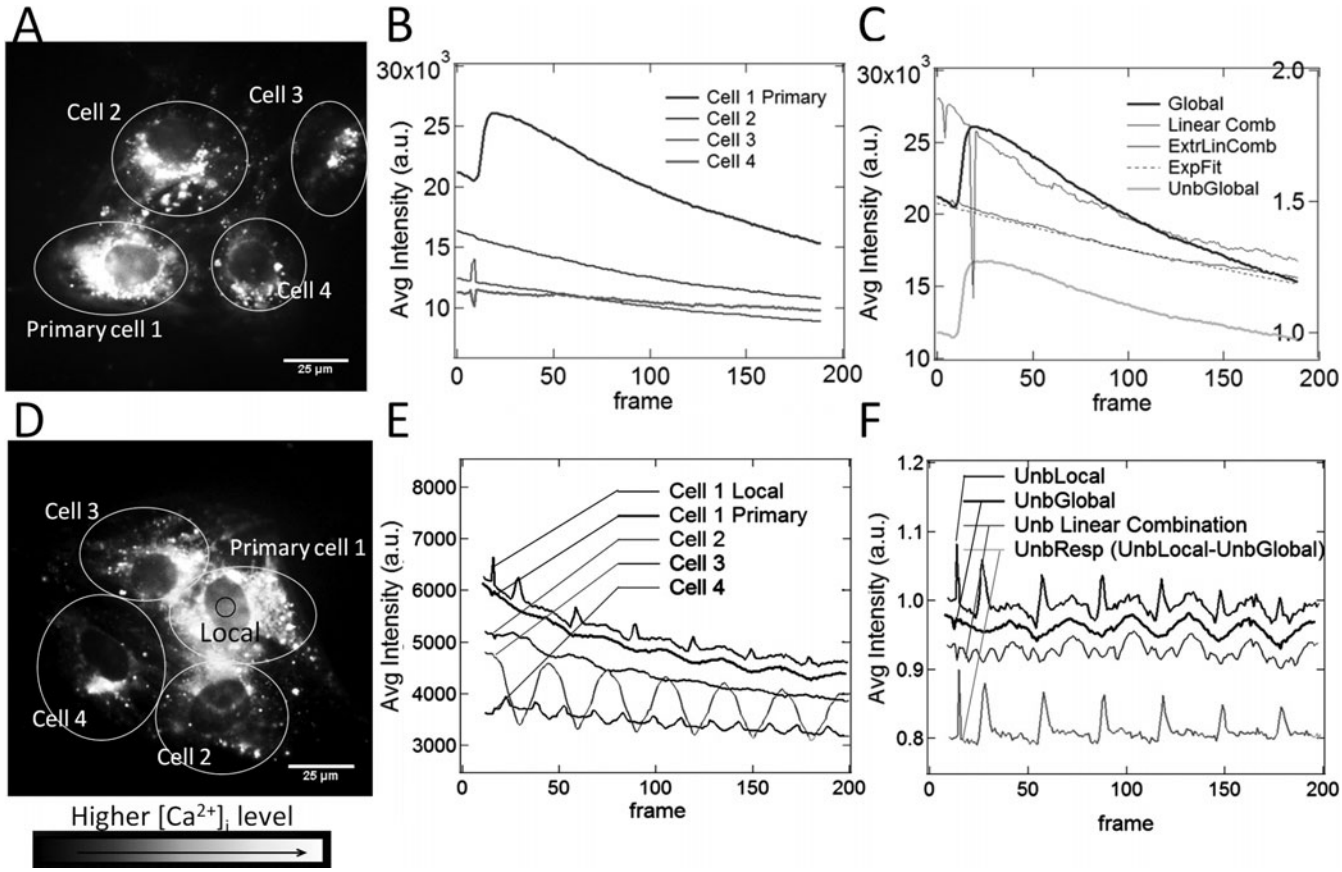

Figure 4. Correction of bleaching and cantilever reflection artifacts in Ca^{2+} responses. Osteoblastic cells were loaded with Fluo4 AM and $[Ca^{2+}]_i$ changes in response to AFM-induced mechanical stimulations were assessed. **A–C:** A single high level indentation leading to membrane penetration was performed, and fluorescence intensity was recorded at ~3 frames/s. **A:** With the assistance of bright-field imaging, the cells in the field of view were identified for analysis as (1) Primary cell 1, which was subjected to AFM indentation, and (2) nonstimulated cells 2–4. **B:** The average fluorescence intensity in each of the selected regions (white ellipses in panel **A**) was plotted as a function of frame. **C:** The linear combination of nonstimulated cells (Linear Comb) was fitted to the Global Ca^{2+} response trace of the Primary cell (Global), or to the initial (before stimulation) and final (last 25 frames of recording) segments of the Global response trace (ExtrLinComb). An exponential fit (Exp. fit) of the later curve was calculated. The Global response trace was divided by the calculated exponential fit resulting in the bleaching-corrected Global response trace (UnbGlobal). **D–F:** Multiple consecutive indentations inducing low level deformation of the cell membrane were performed in the single cell (Primary) and fluorescence intensity was recorded at 3 frames/s. **D:** With the assistance of bright-field imaging, the cells in the field of view were identified for analysis as (1) Primary cell 1, which was subjected to AFM indentation and (2) nonstimulated cells 2–4 (regions of interest are shown as white ellipses). An additional Local region (black circle) was selected as a 5 μm diameter circle centered at the site of indentation. **E:** The average fluorescence intensity of the selected regions (white ellipses and black circle in panel **D**) was plotted as a function of frame. **F:** The linear combination of nonstimulated cells was fitted to the Global response trace, an exponential fit of this curve was calculated, and the traces of global response, local response, and linear combination of nonresponding cells were divided by the calculated exponential fit resulting in unbleached traces (UnbLocal = unbleached local response, UnbGlobal = unbleached global response, Unb Linear Combination = unbleached linear combination of nonresponding cells). To isolate reflection artifacts, the global response was subtracted from the local response resulting in the bleaching and reflection-corrected Local response trace (UnbResp).

In addition to the spatially-averaged fluorescence intensity profile over the whole cells in the field of view (Fig. 4D, white circles), we took the spatially-averaged intensity over a circle of 5 μm in diameter centered on the point of indentation (Local) (Fig. 4D, black circle). To correct for photobleaching, the linear combination $(\sum_{i=2}^{n=1} a(i) \cdot Cell(i))$ of traces from nonstimulated cells was calculated and approximated with a mono-exponential decay curve. The Primary Global and Local traces, as well as the linear combination, were corrected for bleaching by dividing them by the mono-exponential decay curve. Once corrected for bleaching, the Local (Fig. 4F, UnbLocal), the Global (Fig. 4F, UnbGlobal), and the linear combination (Fig. 4F, UnbLinearCombination) profiles were compared. Although we observed oscillatory changes in fluorescence intensity of Global profile, they were similar to oscillations in the linear combination trace

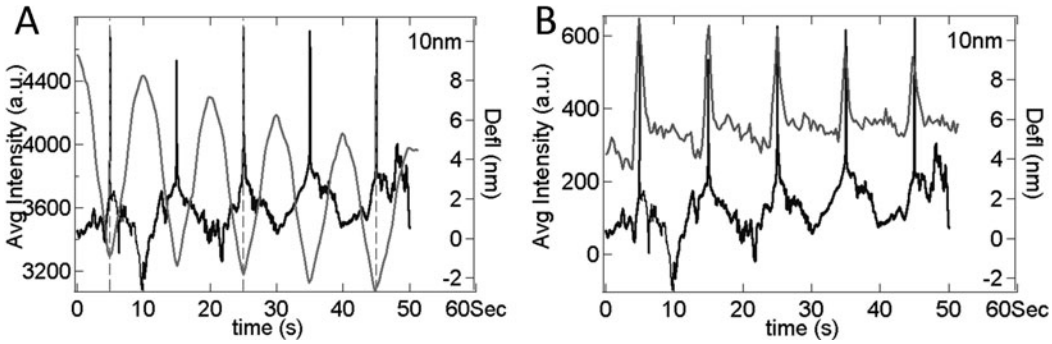

Figure 5. The reflection time stamp in the fluorescence recording can be used to correlate it with the force-spectroscopy measurements. Osteoblastic cells were loaded with Fluo4 AM and changes in $[Ca^{2+}]_i$ in response to multiple consecutive mechanical stimulations of a single cell were assessed. **A:** The average fluorescent intensity of a nonindented cell (gray trace) was overlaid to the force-spectroscopy measurements in the same experiment (black traces) to achieve the best match of fluorescent minima with the points of maximum extensions of the cantilever in a force spectroscopy measurement (dotted lines). **B:** The overlay of bleaching- and reflection-corrected fluorescence trace of a stimulated cell (gray) with the force-spectroscopy measurements (black).

and corresponded to the frequency of mechanical stimulation, allowing us to conclude that the Global Ca^{2+} response is absent; this signal is cantilever displacement induced. However, in the Local fluorescence trace both oscillatory changes present in the Global profile and sharper fluorescence spikes (changes in fluorescence intensity higher than fourfold the average noise) are evident (Fig. 4F). Therefore, we attribute these Local elevations to a cellular Ca^{2+} response to mechanical stimulation. To correct the Local response for illumination artifacts, we subtract the bleaching-corrected Global Ca^{2+} trace (UnbGlobal) from the bleaching-corrected Local Ca^{2+} trace (UnbLocal), resulting in bleaching- and reflection-corrected Local Ca^{2+} response (Fig. 4F, UnbResp).

Using the Cantilever Reflection as a Means to Correlate the Force and Fluorescence Signals

Although both deflection-distance data and fluorescence sequences can be time stamped, different programs are used for data collection, which may be operated on different computers, resulting in uncertainty with the small offsets between the indentation and fluorescence measurements. The presence of cantilever reflection within the fluorescence dataset allows for precise alignment of these independent datasets. Using Igor Pro software the deflection-time traces (Fig. 5A, black) and the fluorescence trace of the nonstimulated cell that exhibited the most prominent oscillations were plotted on the same graph (Fig. 5A, gray), matching the specific events in the deflection-time curves (the time between the maximum deflections for curves one and five), to specific positions in the fluorescence trace (the first and the fifth minima in the fluorescence trace). This procedure allows the temporal component of the fluorescence recording of the stimulated cell to be overlaid with the force spectroscopy measurements (Fig. 5B).

Conclusion

Fluorescence is one of the most common optical techniques used for the characterization and quantification of biological systems. Combining fluorescence measurements with other microscopy techniques allows achieving a better understanding of the molecular and cellular processes. However, it is important to understand potential coupling of signals from the different instruments and be prepared for the possibility of resultant artifacts in the measurements. We have used the combination of AFM microindentation with fluorescence measurements of cytosolic free Ca^{2+} levels. In our experimental setup, the motion of the AFM cantilever with respect to the sample resulted in reflection of light back to the sample and thus changes in the fluorescence intensity profiles that were not related to changes in intracellular calcium levels. We developed a protocol to correct the fluorescence traces for this coupling artifact. In addition, we demonstrate that the coupling of the different tools, when corrected for artifacts, can in fact be used for advanced data analysis, such as more precise temporal correlation of AFM and fluorescence measurements.

Acknowledgments

The authors are grateful to M. Murshed for the C2C12-BMP-2 cell line. The authors thank O. Maria, S. Xing, and G. Sadvakassova for their help providing the cell cultures used in this study. The authors also thank H. Bourque, G. Brouhard, and W. Reisner for helpful discussions. G.M.L.A. was supported by the Principal's Graduate Fellowship, Chalk-Rowles Fellowship, NSERC Graduate Excellence Fellowship, and McGill University. S.V.K. holds Canada Research Chair. This work was supported by Natural Sciences and Engineering Research Council of Canada Discovery grants to S.V.K. and P.H.G.

References

Barfoot, R.J., Sheikh, K.H., Johnson, B.R.G., Colyer, J., Miles, R.E., Jeuken, L.J.C., Bushby, R.J. & Evans, S.D. (2008). Minimal F-actin cytoskeletal system for planar supported phospholipid bilayers. *Langmuir* **24**(13), 6827–6836.

Charras, G.T. & Horton, M.A. (2002). Single cell mechanotransduction and its modulation analyzed by atomic force microscope indentation. *Biophys J* **82**(6), 2970–2981.

Chen, N.X., Ryder, K.D., Pavalko, F.M., Turner, C.H., Burr, D.B., Qiu, J. & Duncan, R.L. (2000). Ca(2+) regulates fluid shear-induced cytoskeletal reorganization and gene expression in osteoblasts. *Am J Physiol-Cell Physiol* **278**, C989–C997.

Duncan, R.L. & Turner, C.H. (1995). Mechanotransduction and the functional response of bone to mechanical strain. *Calc Tissue Int* **57**, 344–358.

Ehrlich, PJ. & Lanyon, LE. (2002). International review article mechanical strain and bone cell function: A review. *Transformation* **13**(9), 688–700.

Guo, X.E., Takai, E., Jiang, X., Xu, Q., Whitesides, G.M., Yardley, J.T., Hung, C.T., Chow, E.M., Hantschel, T. & Costa, K.D. (2006). Intracellular calcium waves in bone cell networks under single cell nanoindentation. *Mol Cell Biomechan* **3**, 95–107.

Hung, C.T., Allen, F.D., Pollack, S.R. & Brighton, C.T. (1996). Intracellular Ca2+ stores and extracellular Ca2+ are required in the real-time Ca2+ response of bone cells experiencing fluid flow. *J Biomechan* **29**, 1411–1417.

Hung, C.T., Pollack, S.R., Reilly, T.M. & Brighton, C.T. (1995). Real-time calcium response of cultured bone cells to fluid flow. *Clin Orthop Relat R* **313**, 256–269.

Kemeny-Suss, N., Kasneci, A., Rivas, D., Afilalo, J., Komarova, S.V., Chalifour, L.E. & Duque, G. (2009). Alendronate affects calcium dynamics in cardiomyocytes *in vitro*. *Vasc Pharmacol* **51**, 350–358.

Li, J., Khavandgar, Z., Lin, S.-H. & Murshed, M. (2011). Lithium chloride attenuates BMP-2 signaling and inhibits osteogenic differentiation through a novel WNT/GSK3-independent mechanism. *Bone* **48**, 321–331.

Molecular Devices (2010). Comparison of the Ca 2 + sensitive dyes Fluo-3 and Fluo-4 used with the FLIPR® Fluorometric Imaging Plate Reader System. Available at: http://www.moleculardevices.com/Documents/general-documents/mkt-appnotes/flipr-appnotes/FLIPR_App_Note_Fluo-3_1_rev_B.pdf.

Molecular Probes (2011). Fluo calcium indicators, product information. Available at: http://probes.invitrogen.com/media/pis/mp01240.pdf.

Muller, D.J. (2008). AFM: A nanotool in membrane biology. *Biochemistry* **47**, 7986–7998.

Oh, Y.J., Jo, W., Lim, J., Park, S., Kim, Y.S. & Kim, Y. (2008). Micropatterning of bacteria on two-dimensional lattice protein surface observed by atomic force microscopy. *Ultramicroscopy* **108**(10), 1124–1127.

Sanchez, H., Kanaar, R. & Wyman, C. (2010). Molecular recognition of DNA-protein complexes: A straightforward method combining scanning force and fluorescence microscopy. *Ultramicroscopy* **110**(7), 844–851.

Vicente, N.B., Zamboni, J.E.D., Adur, J.F., Paravani, E.V. & Casco, V.H. (2007). Photobleaching correction in fluorescence microscopy images. *J Phys Conf Ser* **90**, 012068.